nrp Nutrition Research and Practice

Original Research

Check for updates

Animal protein hydrolysate reduces visceral fat and inhibits insulin resistance and hepatic steatosis in aged mice

Su-Kyung Shin [ID] [1,2], Ji-Yoon Lee [ID] [1,2], Heekyong R. Bae [ID] [1,2], Hae-Jin Park [ID] [3§], and Eun-Young Kwon [ID] [1,2,4§]

[1]Department of Food Science and Nutrition, Kyungpook National University, Daegu 41566, Korea
[2]Center for Food and Nutritional Genomics Research, Kyungpook National University, Daegu 41566, Korea
[3]Bio Convergence Testing Center, Daegu Haany University, Gyeongsan 38610, Korea
[4]Center for Beautiful Aging, Kyungpook National University, Daegu 41566, Korea

[lock] OPEN ACCESS

§**Corresponding Author:**

Hae-Jin Park
Bio Convergence Testing Center, Daegu Haany University, 1 Hanuidae-ro, Gyeongsan 38610, Korea.
Tel. +82-53-819-7876
Fax. +82-53-819-1496
Email. hjpark@dhu.ac.kr

Eun-Young Kwon
Department of Food Science and Nutrition, Kyungpook National University, 80 Daehak-ro, Buk-gu, Daegu 41566, Korea.
Tel. +82-53-950-6231
Fax. +82-53-950-6229
Email. eykwon@knu.ac.kr

ORCID iDs
Su-Kyung Shin [ID]
https://orcid.org/0000-0002-8918-3995
Ji-Yoon Lee [ID]
https://orcid.org/0009-0007-3858-8400

ABSTRACT

BACKGROUND/OBJECTIVES: An increasing life expectancy in society has burdened healthcare systems substantially because of the rising prevalence of age-related metabolic diseases. This study compared the effects of animal protein hydrolysate (APH) and casein on metabolic diseases using aged mice.

MATERIALS/METHODS: Eight-week-old and 50-week-old C57BL/6J mice were used as the non-aged (YC group) and aged controls (NC group), respectively. The aged mice were divided randomly into 3 groups (NC, low-APH [LP], and high-APH [HP] and fed each experimental diet for 12 weeks. In the LP and HP groups, casein in the AIN-93G diet was substituted with 16 kcal% and 24 kcal% APH, respectively. The mice were sacrificed when they were 63-week-old, and plasma and hepatic lipid, white adipose tissue weight, hepatic glucose, lipid, and antioxidant enzyme activities, immunohistochemistry staining, and mRNA expression related to the glucose metabolism on liver and muscle were analyzed.

RESULTS: Supplementation of APH in aging mice resulted in a significant decrease in visceral fat (epididymal, perirenal, retroperitoneal, and mesenteric fat) compared to the negative control (NC) group. The intraperitoneal glucose tolerance test and area under the curve analysis revealed insulin resistance in the NC group, which was alleviated by APH supplementation. APH supplementation reduced hepatic gluconeogenesis and increased glucose utilization in the liver and muscle. Furthermore, APH supplementation improved hepatic steatosis by reducing the hepatic fatty acid and phosphatidate phosphatase activity while increasing the hepatic carnitine palmitoyltransferase activity. Furthermore, in the APH supplementation groups, the red blood cell (RBC) thiobarbituric acid reactive substances and hepatic H_2O_2 levels decreased, and the RBC glutathione, hepatic catalase, and glutathione peroxidase activities increased.

CONCLUSIONS: APH supplementation reduced visceral fat accumulation and alleviated obesity-related metabolic diseases, including insulin resistance and hepatic steatosis, in aged mice. Therefore, high-quality animal protein APH that reduces the molecular weight and enhances the protein digestibility-corrected amino acid score has potential as a dietary supplement for healthy aging.

Keywords: Proteins; aging; visceral fat; insulin resistance; fatty liver; obesity

Nutrition Research and Practice

Heekyong R. Bae [ID]
https://orcid.org/0000-0003-2205-9700
Hae-Jin Park [ID]
https://orcid.org/0000-0002-4283-0809
Eun-Young Kwon [ID]
https://orcid.org/0000-0001-8357-9158

Conflict of Interest
The authors declare no potential conflicts of interests.

Author Contributions
Formal analysis: Lee JY; Investigation: Park HJ; Supervision: Kwon EY; Writing - original draft: Shin SK; Writing - review & editing: Bae HR.

INTRODUCTION

Aging is marked by a general decline in cellular function and is accompanied by DNA damage, oxidative stress, and metabolic dysfunction. It is a gradual and irreversible physiological process characterized by diminishing tissue and cell functions. This process occurs as damage accumulates in response to various stress factors. Ultimately, aging leads to physical and mental illnesses, as well as chronic diseases, such as Parkinson's disease, Alzheimer's disease, obesity, type 2 diabetes mellitus (T2DM), and atherosclerosis [1]. These diseases often influence each other, given that aging is a common risk factor for most metabolic diseases. The increasing life expectancy in society has placed a substantial burden on healthcare systems because of the rising prevalence of age-related metabolic diseases.

The increased life expectancy is accompanied by additional vulnerability to chronic diseases in the elderly, which are associated with obesity. During the aging process, fat is redistributed from the subcutaneous to visceral depots, liver, muscles, and other ectopic sites [2]. These characteristics can lead to insulin resistance and metabolic syndrome through lipotoxicity [3]. Specifically, the increase in visceral fat commonly observed during aging is a major contributor to insulin resistance and metabolic syndrome [4]. Therefore, elderly individuals who become obese as their fat cells enlarge are at an increased risk of metabolic syndrome compared to younger individuals (under 20 yrs old) with the same obesity status [5].

Dysregulation of the hepatic lipid metabolism can also play a central role in the onset of metabolic syndrome. Hepatic steatosis is associated with age-related chronic liver diseases, and its primary characteristic is fat accumulation within liver cells [6]. McGarry [7] proposed that the increased synthesis of hepatic lipids leads to insulin resistance. Specifically, T2DM, a global health problem, is influenced by obesity, particularly in older adults [1]. Elevated levels of plasma free fatty acids (FFAs) and glucose caused by obesity lead to the accumulation of reactive oxygen species (ROS), endoplasmic reticulum stress, and mitochondrial dysfunction, which hinder the proliferation of beta cells [8,9]. As aging progresses, various chronic diseases can mutually influence and co-occur.

Many studies have indicated a positive impact of protein supplementation on muscle health in old age [10,11]. On the other hand, research on the effects of protein supplementation on metabolic conditions in old age is limited. Furthermore, while some reports suggest that animal-based protein quality is superior to plant-based protein, among various animal-based proteins, most supplements primarily use casein [12,13]. Therefore, additional research is needed to understand the qualitative differences in animal-based proteins and their impact on elderly health. Among high-quality protein sources, chicken meat has a higher content of essential amino acids, such as lysine, methionine, and tryptophan, compared to other meats. Therefore, chicken breast meat was hydrolyzed to increase the Protein Digestibility-Corrected Amino Acid Score (PDCAAS), reduce molecular weight, and enhance the functionality of animal-based protein supplements that can potentially benefit the elderly. As shown in **Table 1**, the commercial casein used as the control group is a mixture of α, β, and κ-casein with molecular weights of 22,068–25,230, 23,944–24,092, and 19,007–19,039, respectively. In contrast, animal protein hydrolysate (APH), which is hydrolyzed from chicken breast, has a molecular weight of approximately 675. APH has much higher PDCAAS at 128.8 than casein (98.34). On the other hand, there was no significant difference in the essential amino acid composition between APH and casein.

Table 1. Average molecular weight and PDCAAS of protein sources

Protein source	Molecular weight	PDCAAS (%)
Casein		98.34 ± 0.55
α	22,068–25,230	
β	23,944–24,092	
κ	19,007–19,039	
APH	675	128.8 ± 0.85

PDCAAS, Protein Digestibility-Corrected Amino Acid Score; APH, animal protein hydrolysate.

This study compared the quantities of APH and casein in aged mice to determine the effects of PDCAAS and the differences in the molecular weight of animal proteins on metabolic disorders. Specifically, the effects of APH in relation to age-related diseases, such as obesity, fatty liver, and insulin resistance, were assessed.

MATERIALS AND METHODS

Materials and preparation of APH

Chicken breast and enzymes were purchased in 2021 from Kyochon F&B Co., Ltd. and Vision Biochem Co., Ltd. The chicken breast was sliced, pulverized, and subjected to enzymatic hydrolysis under specific conditions, including alkaline protease, prozyme 2000P, bromelain, and papain. After the enzymatic reaction, the enzyme activity was deactivated by heating. The sample was then filtered, concentrated, sterilized, and spray-dried to obtain the final product with a Brix value of 15–20.

Molecular weight and PDCAAS assessment of APH

The protein molecular weight was analyzed. A 0.1 g sample was mixed with 10 mL of deionized water and sonicated for 10 min. After cooling, the solution concentration was adjusted to 4 mg/mL with deionized water, filtered through a 0.45 μm polyvinylidene fluoride syringe filter, and analyzed by high-performance liquid chromatography with polyethylene glycol as the standard. Gel permeation chromatography was conducted on a Shodex column and 0.1 M $NaNO_3$ as the mobile phase, operating at a flow rate of 0.8 mL/min and an injection volume of 80 μL. PDCAAS was calculated using the method reported by Schaafsma [14], and the formula is as follows:

PDCAAS (%) = Amino Acid Score (AAS) × TPD (%)

AAS = Contents of Limiting Amino Acid in Test Protein (mg/g)/Contents of the Same Amino Acid in Reference Protein (mg/g)

Table 1 lists the molecular weights and PDCAAS measurement results for casein and APH.

Animals and diet

In this study, 24 male aged mice (C57BL/6J, 50 weeks old) and nine male young mice (C57BL/6J, 8 weeks old) were obtained from JA Bio (Suwon, Korea). All mice were kept under controlled conditions (12-h light-dark cycle, 25°C, 40–60% humidity) and underwent an adaptation period. The aged mice were divided into 3 groups: Negative control (NC) group (n = 8, with protein calories from casein at 16% of total energy), low-dose APH-supplemented (LP) group (n = 8, with protein calories from APH at 16% of total energy), and high-dose APH-supplemented (HP) group (n = 8, with protein calories from APH at 24% of the total energy). Dietary compositions were adjusted based on the casein and APH contents. In addition, 8-week-old mice were used as a young control (YC) group. All mice were fed their respective

diets ad libitum for 12 weeks. The animal experiment procedures complied with the protocols approved by the Institutional Animal Care and Use Animal Ethics Committee (DHU 2022-055).

Sample preparation

At the end of the experimental period, all mice were sacrificed with isoflurane (5 mg/kg body weight; Urim Pharm, Daejeon, Korea) after a 12-h fast. Blood samples were collected into heparin-coated tubes from the inferior vena cava to analyze biomarkers. The collected blood samples were processed into plasma samples by centrifugation at 1,000 ×g for 15 minutes at 4°C. After separating plasma from blood, it was stored in a deep freezer. The liver, muscle, and adipose tissue were promptly removed, rinsed with physiological saline, and weighed. After tissue removal, they were frozen immediately in liquid nitrogen and stored at −70°C.

Lipid profiles in plasma and tissues

The plasma levels of total cholesterol (TC), triglycerides (TG), and high-density lipoprotein cholesterol (HDL-C) were determined using enzyme kits from Asan Pharm Co. (Seoul, Korea). The FFAs were quantified using a separate enzyme kit. The lipids were extracted from the tissue by dissolving dried lipid residues with 1 mL of ethanol. Emulsification was performed by adding 200 μL of an emulsifier containing Triton X-100 and sodium cholate in distilled water to the dissolved lipid solution. Cholesterol, TG, and fatty acids were measured using the same enzyme kit used for the plasma analysis.

Fasting blood glucose concentration and intraperitoneal glucose tolerance test (IPGTT)

The blood glucose concentrations were measured following a 12-h fast every 4 weeks over a 12-week period. An IPGTT was conducted during the 10th week. After a 12-h fast, all mice received intraperitoneal glucose injections, and the blood glucose levels were measured at 0, 30, 60, and 120 min.

Plasma insulin and glucagon

The plasma insulin levels were measured using a Mouse Insulin ELISA Kit (ThermoFisher Scientific, Waltham, MA, USA). The plasma glucagon levels were determined using the Glucagon Immunoassay Quantikine ELISA Kit (R&D Systems, Minneapolis, MN, USA).

Glycogen analysis in hepatic and muscle tissue

The glycogen concentration was determined using a slight modification of the method described by Carroll et al. [15]. For glycogen in the liver and gastrocnemius muscle tissues, 80 μL of 30% KOH was added after tissue extraction. After heating at 100°C for 30 min, 200 μL of 95% ethanol was added, followed by overnight incubation at 4°C. The pellet generated by centrifugation was dissolved in 1 mL of distilled water. Anthrone reagent was then added and heated at 100°C for 20 min. The glycogen concentration was measured at an absorbance of 620 nm.

Glucose-related enzyme activity analysis

The phosphoenolpyruvate carboxykinase (PEPCK) activity was assessed by measuring the rate of oxaloacetate synthesis and the reduction of NADH to NAD, according to the spectrophotometric assay developed by Bentle and Lardy [16]. The glucose 6-phosphatase (G-6-pase) activity was determined based on the method described by Alegre et al. [17] with slight modifications. The glucokinase (GK) activity in the cytosol was measured using a spectrophotometric assay described by Davidson and Arion [18].

Lipid-regulated enzyme activities in the liver

The ME activity was assessed by measuring nicotinamide adenine dinucleotide phosphate (NADPH) production in the cytosol. The assay was initiated by adding 600 μL of 0.4M triethanolamine buffer to the tube, followed by the sequential addition of reagents: 30 nM L-malate, 0.12 M MnCl, and 3.4 nM TPN. The absorbance was measured at 340 nm. The fatty acid synthase (FAS) activity was determined in the cytosol using the method outlined by Nepokroeff *et al.* [19]. The phosphatidate phosphatase (PAP) activity was measured in microsomes. Reagent A (0.05 M Tris-HCl, 1.25 mM ethylenediaminetetraacetic acid, and 1 mM MgCl) and reagent B (1.8 M H_2SO_4, sodium dodecyl sulfate, ascorbic acid) were added, and the absorbance was measured at 820 nm. The carnitine palmitoyltransferase (CPT) activity in the mitochondria was measured according to the protocol described by Markwell *et al.* [20]. Fatty acid β-oxidation was measured spectrophotometrically by monitoring the reduction of NAD to NADH in the presence of palmitoyl-CoA, as described by Lazarow [21].

Hydrogen peroxide and lipid peroxide measurement in the liver

The hydrogen peroxide content was assessed using Wolff's method, with absorbance readings taken at 560 nm. The lipid peroxide content was determined using the method outlined by Ohkawa *et al.* [22], and the absorbance of the supernatant after centrifugation was measured at 532 nm.

Antioxidant enzyme activity analysis

The superoxide dismutase (SOD) activity was determined using the autoxidized pyrogallol reagent based on the method described by Marklund and Marklund [23]. The chloramphenicol acetyltransferase enzyme activity, which decomposes H_2O_2 into H_2O and O_2, was assessed using the method reported by Aebi [24]. The glutathione peroxidase (GSH-Px) activity was measured using a slight modification of the method reported by Paglia and Valentine [25]. The glutathione reductase (GR) activity was determined using a slight modification of Pinto's method to measure the extent of NADPH reduction [26]. The paraoxonase (PON) activity was assessed using the method described by Graham *et al.* [27].

Fecal lipid profile analysis

After pulverizing the feces, 0.3 g was placed into a tube, and 3 mL of chloroform-ethanol (2:1) was added. The mixture was vortexed and left to stand at 4℃ for 24 h. After centrifugation, the supernatant was carefully collected, dried with nitrogen gas, and re-dissolved in 1 mL of chloroform-ethanol (2:1) through sonication. Subsequently, the triglyceride and cholesterol contents were determined using the same kit for plasma analysis.

Gene expression levels

After extracting the total RNA from gastrocnemius muscle and liver tissues, reverse transcription was conducted to synthesize the cDNA from the RNA samples. Subsequently, the samples were diluted with diethylpyrocarbonate, and mRNA expression analysis was performed using TB Green® Premix EX Taq™ II on a CFX96™ Real-Time Detection System (Bio-Rad, Hercules, CA, USA). **Table 2** lists the primers for the genes. The cycle threshold values were normalized using glyceraldehyde 3-phosphate dehydrogenase as a reference.

Histological and immunohistochemistry analysis

The liver and white adipose tissues (WAT) removed from the mouse were fixed with a 10% formalin solution buffer. The fixed samples were embedded in paraffin, cut to a 5 μm thickness, and stained with hematoxylin and eosin stain (H&E) and Masson's trichrome

Table 2. Primer sequences for real-time PCR

Primer	Sequence (5′-3′)
AKT	F: ACG TGG TGA ATA CAT CAA GAC C
	R: GCT ACA GAG AAA TTG TTC AGG GG
ALDOA	F: GTG GGA AGA AGG AGA ACC TG
	R: CTG GAG TGT TGA TGG AGC AG
CREB	F: GAA GAA GCA GCA CGG AAG AGA
	R: TCT CTT GCT GCC TCC CTG TT
GAPDH	F: TGC AGT GGC AAA GTG GAG AT
	R: TTG AAT TTG CCG TGA GTG GA
GLUT4	F: CTG AGA ACT TAA CTG CTG AAG
	R: AGG AGT TTG TTG GTG TAT TTA
GPI1	F: CGG AAA GGT CTG CAT CAC AA
	R: CCT TCA TCA GGG CCT CAG TC
GLUT2	F: GTC AGA AGA CAA GAT CAC CGG A
	R: AGG TGC ATT GAT CAC ACC GA
HK2	F: GAG AAC CGT GGA CTG GAC AA
	R: CCA GGA AGG ACA CGT ACAC AT
PDHB	F: CAT CTC GTG ACT GTG AAA GGA G
	R: A TCA GCA CCA GTG ACA CGC A
PEPCK	F: TGC CTC TCT CCA CAC CAT TGC
	R: TGC CTT CCA CGA ACT TCC TCA C
PKM	F: TTG ACT CTG CCC CCA TCA C
	R: GCA GGC CCA ATG GTA CAA AT
PRKAA2	F: CAG AAG ATT GGC AGT TTA GAT GTT GT
	R: ACC TCC AGA CAC ATA TTC CAT TAC C
PRKAB1	F: GTT GCT GTT GCT TGT TCC AA
	R: ATA CTG TGC CTG CCT CTG CT
PRKAG1	F: TCT CCG CCT TAC CTG TAG TGG A
	R: GCA GGG CTT TTG TCA CAG ACA C

PCR, polymerase chain reaction; AKT, protein kinase B; ALDOA, aldolase A; CREB, cAMP response element-binding protein; GAPDH, glyceraldehyde 3-phosphate dehydrogenase; GLUT4, glucose transporter 4; GPI1, glucose phosphate isomerase 1; GLUT2, glucose transporter 2; PDHB, pyruvate dehydrogenase (lipoamide) β; PEPCK, phosphoenolpyruvate carboxykinase; PKM, pyruvate kinase M2; PRKAA2, 5′-AMP-activated protein kinase subunit alpha-2; PRKAB1, 5′-AMP-activated protein kinase subunit beta-1; PRKAG1, 5′-AMP-activated protein kinase subunit gamma-1.

(MT). The stained tissue was observed using an optical microscope (Zeiss Axio Scope, Oberkochen, Germany).

Statistical analysis

The data were analyzed using the SPSS package program (IBM SPSS Statistics, Chicago, IL, USA). The experimental results are presented as the mean ± standard error of the mean. For the comparison between the YC and NC groups, a Student's t-test was performed with significance levels indicated as follows: [*]$P < 0.05$, [**]$P < 0.01$, [***]$P < 0.001$. For the comparison between the aged mice group and experimental groups (LP and HP), a Student's t-test was performed with significance levels denoted as follows: [#]$P < 0.05$, P[##] < 0.01, [###]$P < 0.001$. For the comparison among the NC, LP, and HP groups, one-way analysis of variance (ANOVA) followed by Tukey-Test multiple range was conducted. The significant differences between the groups are represented by the superscript lower case letters ([a,b,c]).mean values at $P < 0.05$.

RESULTS

APH supplementation reduced the body fat and plasma lipid profiles

Compared to the YC group, the aging mouse groups had significantly higher body weights from the beginning of the experiment, which remained consistent until the completion

of the study. On the other hand, during the experimental period, the YC group showed a significantly larger increase in body weight gain than the NC (aged mice) group. Supplementation with APH did not influence the weight changes among the aging groups (**Fig. 1A and B**). The food and energy intake increased significantly in the NC group compared to the YC group. In contrast, the food efficiency ratio (FER) showed a significant decrease (**Fig. 1C**). A comparison of the aged mice groups revealed the food and energy intake to be significantly lower in the APH-supplemented groups (the LP and HP groups) than the NC group, but there was no significant difference in the FER among the aged mice groups.

The weights of the representative WAT, including epididymal fat, perirenal fat, retroperitoneum fat, and mesenteric fat, were significantly higher in the NC group than the YC group, resulting in a significantly higher amount of visceral fat in the NC group (**Fig. 1D**). The interscapular WAT (iWAT) was also higher in the NC group than the YC group. In contrast, the brown adipose tissue exhibited a significant decrease. Supplementation of APH in aging mice resulted in a decrease in the epididymal, perirenal, and mesenteric fat weights and iWAT compared to the NC group. This effect significantly decreased the visceral and total WAT in the APH-treated groups compared to the NC group, with the LP group showing the lowest levels (**Fig. 1D**).

Morphological analysis of the epididymal WAT showed that the adipocyte size was significantly larger in the NC group than in the YC group. In contrast, the APH supplementation group showed a significant decrease in adipocyte size (**Fig. 1E**). MT staining of the epididymal WAT revealed a significant increase in the fibrotic areas due to aging, which was reduced dramatically by APH supplementation (**Fig. 1E**).

APH supplementation in aged mice significantly reduced the plasma total cholesterol (TC) and non-HDL-C levels. The plasma FFA level was significantly higher in the NC group than in the YC group, and the HDL-C/TC ratio (HTR) was significantly lower. There were no significant changes in plasma TG, FFA, HDL-C, and HTR levels due to the administration of APH, but they showed a similar trend to the YC group.

APH supplementation ameliorated insulin resistance

The fasting blood glucose concentration was measured every four weeks during the experimental period. The fasting blood glucose concentrations in the NC group were significantly higher than in the YC group in the fourth, eighth, and 12th weeks. In addition, there was no significant difference in the 4th and 8th weeks among the aged mice groups. At week 12, the LP and HP groups showed a significantly lower fasting blood glucose concentration than the NC group (**Fig. 2A**). The intraperitoneal glucose tolerance test and area under the curve (AUC) analysis revealed insulin resistance in the NC group, which was alleviated by APH supplementation (**Fig. 2B**). The plasma glucose and insulin concentrations in the NC group were significantly higher than in the YC group and tended to decrease with APH supplementation. The plasma glucagon level tended to increase in the NC group compared to the YC group, and the plasma glucagon level was significantly lower in the HP group than in the NC group (**Fig. 2C**). The hepatic glycogen contents were significantly increased in the NC group compared to the YC group, and significantly decreased in HP group compared to the NC group.

The hepatic PEPCK and G-6-pase activities, which are gluconeogenesis-related enzyme activities, were significantly higher in the NC group than in the YC group. The hepatic GK
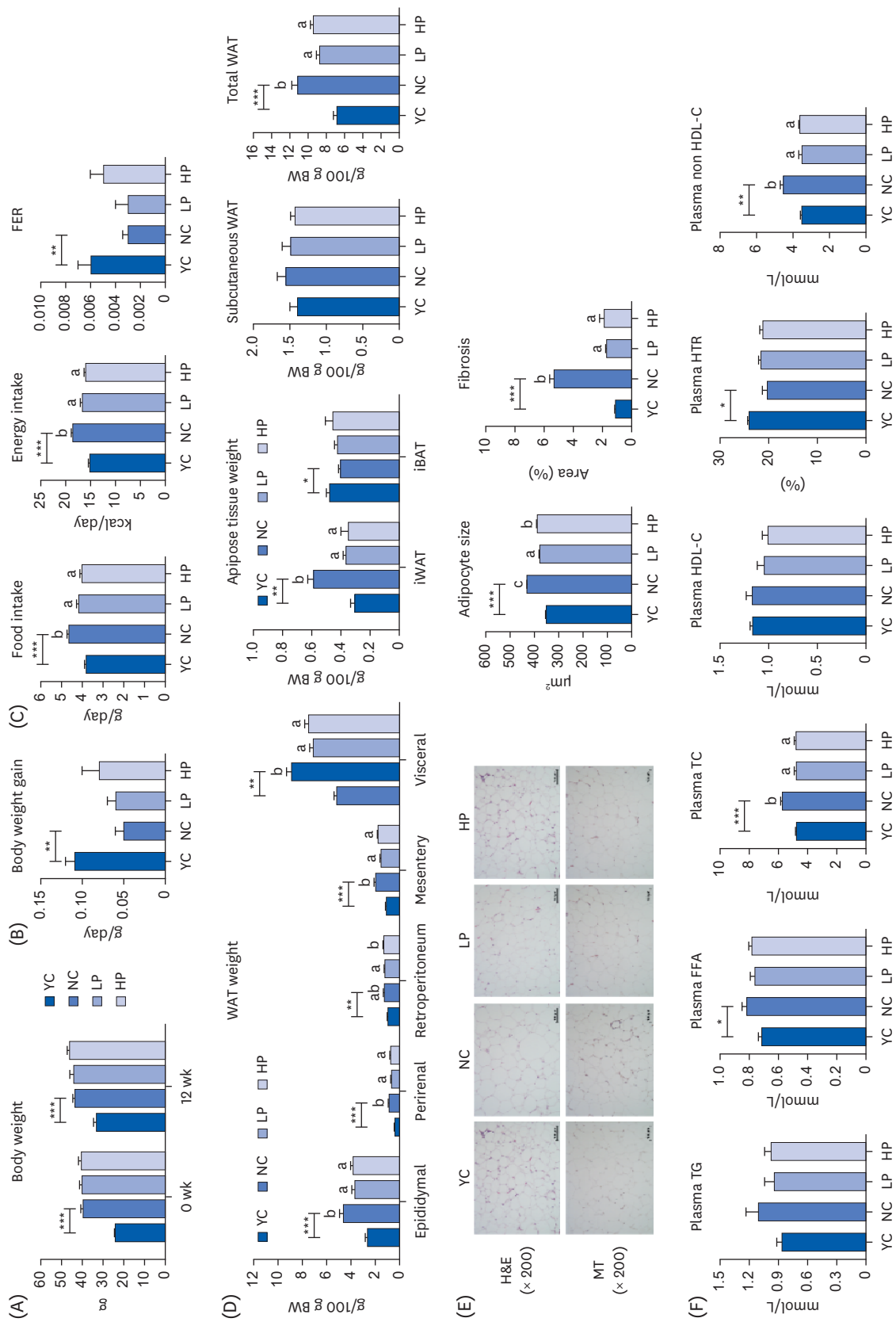
Fig. 1. Effect of APH on body weight (A), body weight gain (B), food intake; energy intake; FER (C), WAT weight (D), Representative images for H&E and MT staining of epididymal fat (E), plasma lipid profiles (F) in aged mice. The data are expressed as the mean ± SEM; Student's t-test (n = 4–8).

APH, animal protein hydrolysate; FER, food efficiency ratio; WAT, white adipose tissues; H&E, hematoxylin and eosin stain; MT, Masson's trichrome; SEM, standard error of the mean; YC, young control; NC, negative control (casein 16% of total energy); LP, low-APH (APH 16% of total energy); HP, high-APH (APH 24% of total energy); TG, triglyceride; FFA, free fatty acid; TC, total cholesterol; HDL-C, high-density lipoprotein cholesterol; HTR, HDL-C/TC ratio.

* $P < 0.05$, ** $P < 0.01$, *** $P < 0.001$ versus YC group.

[a,b]Means not sharing a common letter are significantly different among the old mice groups at $P < 0.05$.
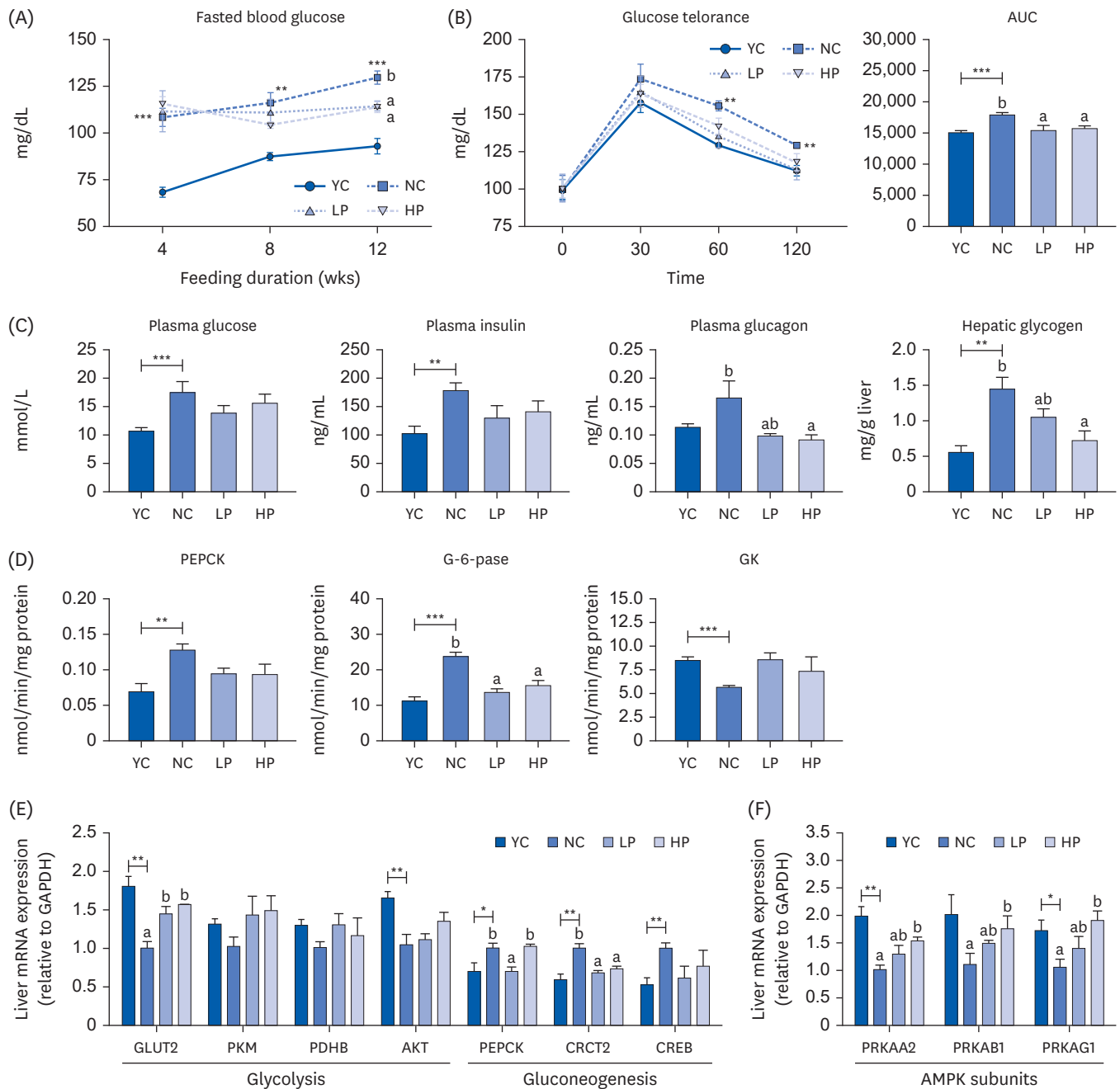
Fig. 2. Effect of APH on the weekly fasted blood glucose (A), IPGTT; AUC (B), plasma glucose; insulin; glucagon; hepatic glycogen (C), activities of hepatic glucose-regulating enzyme on liver (D), mRNA expression related to glucose metabolism on the liver (E), mRNA expression of AMPK subunit (F) in aged mice. The data are expressed as the mean ± SEM; Student's t-test (n = 4–8).

APH, animal protein hydrolysate; IPGTT, intraperitoneal glucose tolerance test; AUC, area under the curve; AMPK, AMP-activated protein kinase; SEM, standard error of the mean; YC, young control; NC, negative control (casein 16% of total energy); LP, low-APH (APH 16% of the total energy); HP, high-APH (APH 24% of the total energy); PEPCK, phosphoenolpyruvate carboxykinase; G-6-pase, glucose-6-phosphatase; GK, glucokinase; GLUT2, glucose transporter 2; PKM, pyruvate kinase M2; PDHB, pyruvate dehydrogenase (lipoamide) beta; AKT, protein kinase B; CREB, cAMP response element-binding protein; CRCT2, CREB-regulated transcription coactivator 2; AMPK, 5' AMP-activated protein kinase; PRKA, 5'-AMP-activated protein kinase subunit.

[*]$P < 0.05$, [**]$P < 0.01$, [***]$P < 0.001$ versus YC.

[a,b]Means not sharing a common letter are significantly different among the old mice groups at $P < 0.05$.

activity, a glycolysis-related enzyme, was significantly lower in the NC group than in the YC group. The hepatic PEPCK and GK activities were similar in the old-aged mice. In contrast, the G-6Pase activity was significantly lower in the LP and HP groups than in the NC group (**Fig. 2D**). The hepatic mRNA expression of PEPCK, cAMP response element-binding protein (CREB), and CREB-regulated transcription coactivator 2 (CRTC2), all involved in gluconeogenesis, increased significantly in the NC group compared to the YC group. PEPCK and CRTC2 expression decreased significantly in the LP group, while only CRTC2 expression decreased significantly in the HP group. In the glycolysis process, glucose transporter 2 (GLUT2), enzyme pyruvate kinase M2 (PKM), pyruvate dehydrogenase (lipoamide) beta (PDHB), and Akt were involved. The mRNA expression of GLUT2 decreased significantly due to aging and significantly increased regardless of the APH concentration (**Fig. 2E**). The mRNA expression of 5' AMP-activated protein kinase (AMPK) subunits in the liver was measured. The 5′-AMP-activated protein kinase subunit alpha-2 (PRKAA2), 5′-AMP-activated protein kinase subunit beta-1 (PRKAB1), and 5′-AMP-activated protein kinase subunit gamma-1 (PRKAG1) expression levels were lower in the NC group and were increased by APH supplementation, particularly in the HP group (**Fig. 2F**).

Improved insulin resistance was observed in the liver and the gastrocnemius muscle. There were no differences in the muscle glycogen levels among the groups, but the mRNA expression of PRKAA2 decreased due to aging and tended to restore in the APH groups. In particular, the significant increase in mRNA expression of glucose phosphate isomerase 1 (GPI), 6-phosphofructokinase-muscle type (PFKM), aldolase A (ALDOA), and PKM in the APH supplementation group indicates the activation of pathways that utilize glucose as an energy source (**Supplementary Fig. 1**).

APH supplementation improved hepatic steatosis

The significant increase in liver weight due to aging was reduced significantly in the LP group, and there was a tendency for a decrease in the HP group (**Fig. 3A**). The hepatic TG, FA, and cholesterol levels were significantly higher in the NC group than in the YC group. Compared to the aged mice groups, the LP and HP groups had significantly higher hepatic FA levels than the NC group (**Fig. 3B**). The hepatic activities of the enzymes involved in fatty acid synthesis pathways, malic enzyme (ME), fatty acid synthase (FAS), and PAP were significantly lower in the NC group than in the YC group. Among these, the hepatic PAP activity was significantly lower in the two groups that received the APH treatment. The hepatic activities of CPT and β-oxidation, both involved in the fatty acid oxidation pathways, were significantly lower in the NC group than in the YC group. The CPT activity was significantly higher in the LP group than in the NC group, and there was a tendency for increased β-oxidation activity in the experimental groups (**Fig. 3C**).

The morphological observations suggested that the accumulation of lipid droplets was higher in the NC group than in the YC group. In contrast, the accumulation of lipid droplets was reduced through APH supplementation. MT staining shows a significant increase in fibrosis in the NC group compared to the YC group. On the other hand, it was decreased significantly through APH supplementation (**Fig. 3D**).

The fecal TG level was significantly lower in the NC group than in the YC group. The TG level was significantly higher in the HP group than in the aged mouse group. The fecal cholesterol levels were similar in the young and aged mice, but they were significantly lower in the LP group than in the NC group (**Fig. 3E**).
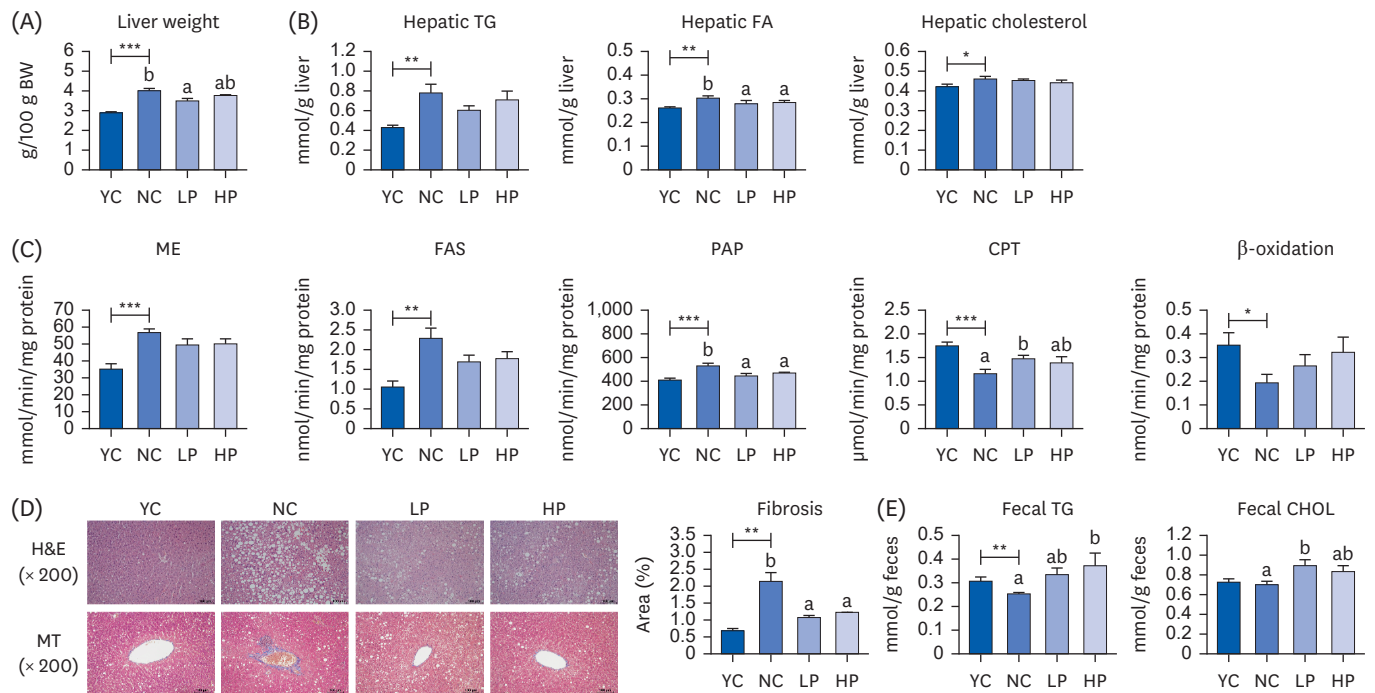
Fig. 3. Effect of APH on the liver weight (A), hepatic lipid profiles (B), activities of hepatic lipid-regulating enzyme (C), Representative images for H&E and MT staining of the liver (D), fecal TG; cholesterol in aged mice. The data are expressed as the mean ± SEM; Student's t-test (n = 4–8).

APH, animal protein hydrolysate; H&E, hematoxylin and eosin stain; MT, Masson's trichrome; TG, triglyceride; SEM, standard error of the mean; YC, young control; NC, negative control (Casein 16% of the total energy); LP, low-APH (APH 16% of the total energy); HP, high-APH (APH 24% of total energy); FA, fatty acid; ME, malic enzyme; FAS, fatty acid synthase; PAP, phosphatidate phosphatase; CPT, carnitine palmitoyltransferase.

*$P < 0.05$, **$P < 0.01$, ***$P < 0.001$ versus YC.

a,bMeans not sharing a common letter are significantly different among the old mice groups at $P < 0.05$.

APH supplementation improved antioxidant metabolism

An additional analysis was conducted using RBC and liver to determine if APH influences the antioxidant defense system. The measurements of thiobarbituric acid reactive substances (TBARS) and H_2O_2 levels, indicators of oxidative stress, revealed an increase in both RBC and liver from the aged mice compared to the young mice (**Fig. 4A**). The TBARS level in the RBC was significantly lower in the LP and HP groups than in the NC group, while TBARS level in the liver was significantly lower only in the LP group. The HP-supplemented group exhibited significantly lower hepatic H_2O_2 levels than the NC group. The plasma SOD activity and RBC GSH levels decreased with aging, but there was no change due to APH administration. The plasma PON activity was increased by APH supplementation (**Fig. 4B**). The activity of antioxidant enzymes SOD, catalase (CAT), and GSH-Px, which directly influence the H_2O_2 concentration, was measured in liver tissue. The activities of SOD, CAT, and GSH-Px were significantly lower in the NC group than in the YC group. On the other hand, in the group treated with LP, there was a significant increase in CAT and GSH-Px activity compared to the NC group. Moreover, although not statistically significant, there was a trend of an increase in the group treated with HP. The activity of GSH and glutathione reductase (GR) did not show changes caused by aging in the liver (**Fig. 4B**).

DISCUSSION

The changes in body fat distribution and metabolism caused by aging are key factors in accelerating the aging process and the onset of age-related diseases [3]. In particular, various
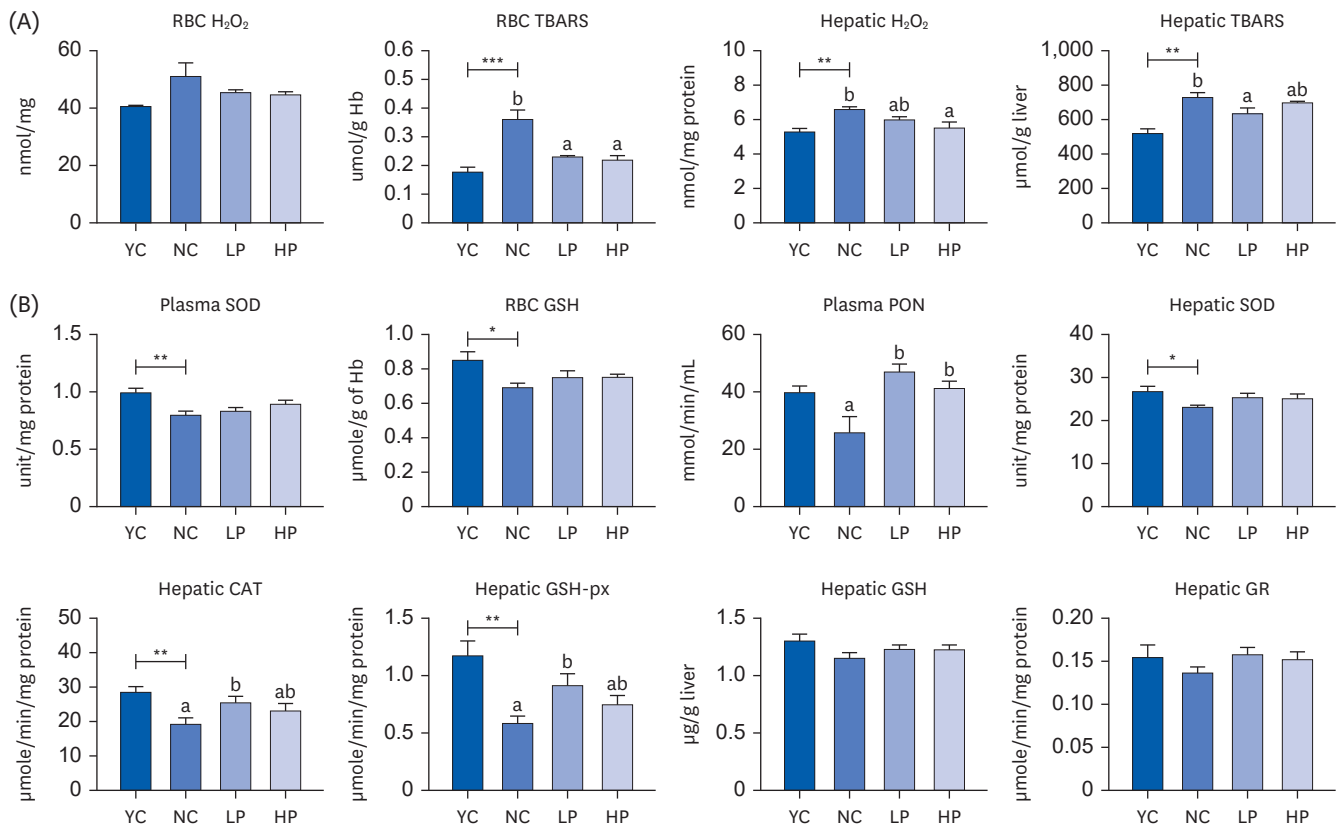
Fig. 4. Effect of APH on RBC H_2O_2 and TBARS; Hepatic H_2O_2 and TBARS (A), activities of plasma and hepatic antioxidant enzyme (B) in aged mice. The data are expressed as the mean ± SEM; Student's *t*-test (n = 4–8).

APH, animal protein hydrolysate; RBC, red blood cell; TBARS, thiobarbituric acid reactive substances; SEM, standard error of the mean; YC, young control; NC, negative control (casein 16% of total energy); LP, low-APH (APH 16% of total energy); HP, high-APH (APH 24% of total energy); SOD, superoxide dismutase; GSH, glutathione; PON, paraoxonase; CAT, catalase; GSH-Px, glutathione peroxidase; GR, glutathione reductase.

[*]$P < 0.05$, [**]$P < 0.01$, [***]$P < 0.001$ versus YC.

[a,b]Means not sharing a common letter are significantly different among the old mice groups at $P < 0.05$.

studies have shown that removing visceral fat can improve insulin resistance and reduce systemic TG, FFA, and hepatic TG levels [28,29]. In this study, APH supplementation in aged mice reduced visceral fat significantly, improving insulin resistance and hepatic steatosis.

The aging process is accompanied by decreased skeletal muscle mass and increased total body fat, especially visceral fat [30]. The skeletal muscle mass typically accounts for approximately 50% of the total body weight in young adults but decreases to approximately 25% by 75–80 years of age [31]. Therefore, as individuals age, the proportion and amount of lean muscle mass decrease while body fat mass increases, representing a key biomarker of aging [30]. In particular, visceral fat accumulation is the most prominent feature of aging in humans [32]. Importantly, aging rodents also show a similar increase in fat mass to aging humans, almost mirroring the pattern [32]. The results of the present study showed that there was no significant difference in body weight among the aging mice. On the other hand, supplementation with APH led to a significant decrease in the amount of WAT, regardless of the dosage. In particular, the epididymal, perirenal, retroperitoneum, and mesentery WAT depots decreased, dramatically reducing visceral fat, a hallmark of aging. These effects are believed to have been influenced by the reduction in the size of adipocytes and fibrosis. Supplementation with APH may help suppress the complications arising from metabolic disorders triggered by visceral fat accumulation during the aging process.

The increase in visceral fat commonly observed during aging is a major contributor to insulin resistance and metabolic diseases [3]. Insulin sensitivity decreases when adipose tissue reaches its storage capacity [33]. In particular, age-related difficulty in expanding adipose tissue makes it more susceptible to ectopic lipid accumulation because adipose tissue can no longer accommodate excess energy storage [34,35]. Consequently, obesity is exacerbated by ectopic lipid accumulation, leading to lipotoxicity and a vicious cycle that ultimately results in the development of insulin resistance and T2DM.

A complex set of mechanisms related to glucose intake and production operates to maintain blood glucose in a stable state. Glucose is transported through the cell membrane by proteins known as glucose transporters. The insulin-regulated GLUT is one of the glucose transporters involved in glycolytic regulation [36]. Glycolysis is a process in which glucose is converted into pyruvate through a 10-step reaction to produce energy. This conversion is achieved by increasing the activity of enzymes, such as GK, phosphofructokinase, and pyruvate kinase in the liver. The glucose utilization increases when glycolysis is enhanced, indirectly reducing the movement of intracellular glucose into the bloodstream [37]. In addition, it inhibits the release of glucose from the cell by reducing the activity of G-6-pase in the liver. On the other hand, glucose production in the liver is carried out primarily through glycogenolysis and gluconeogenesis.

Glucose is absorbed by the target tissues, including skeletal muscles and adipose tissue. One of the characteristics of T2DM is excessive hepatic glucose production [38]. In cases of insulin resistance or T2DM, hepatic glucose metabolism disorders occur within the liver, including increased gluconeogenesis and impairment of enzymes associated with this process [38]. In a state of insulin resistance, the activation of genes required for gluconeogenesis, most notably PEPCK and G-6-pase, is induced [39]. These results showed that PEPCK, G-6-pase, and CRCT2 were down-regulated, while GK and GLUT2 were elevated significantly in the LP and HP groups. Therefore, the increase in hepatic glycogen in aging mice appears to be through gluconeogenesis, and the reduction in hepatic glycogen in the APH group was attributed to increased glucose utilization. Activation of glycolytic pathways (GLUT1, GPI1, PFKM, ALDOA, and PKM) in gastrocnemius muscle was also observed with APH supplementation.

Lipid metabolism imbalance is the most direct cause of hepatic steatosis. The onset of hepatic steatosis occurs due to an imbalance between lipogenesis and lipolysis in the liver. A lipid metabolism imbalance is the most direct cause of hepatic steatosis [40]. More than half of the FFA contributing to liver lipid accumulation is derived from peripheral fat breakdown. Importantly, TG breakdown is mediated by insulin action on adipose tissue. Insulin resistance leads to the excessive production of fatty acids from adipose tissue, contributing to hepatic lipid accumulation [41]. The second major source of hepatic FFA is *de novo lipogenesis* (DNL). Through DNL, hepatic cells convert excessive dietary glucose and fructose into fatty acids [42].

FFA removal can be considered a crucial link in inhibiting hepatic steatosis. In this study, a significant increase in plasma FFA and hepatic FA compared to YC was observed in aged mice, increasing hepatic TG. This is believed to be due to the significant increase in hepatic ME, FAS, and PAP activities in aged mice compared to YC, while CPT activity decreased significantly. High-dose APH supplementation decreased the hepatic FA and PAP activity, and low-dose APH supplementation decreased the hepatic PAP activity and increased the hepatic CPT activity. Therefore, APH supplementation partially helped improve hepatic steatosis.

Lipid metabolism disorders affect hepatic steatosis and influence the generation of various ROS within the hepatic tissue [41]. As evidence, studies have reported increased levels of TBARS in the liver and blood in cases of hepatic steatosis, accompanied by a decrease in hepatic CAT, GSH-Px, and GSH activities [43-45]. The dysfunction of the antioxidant mechanism exacerbates oxidative stress by continuously generating ROS, particularly excessive production of H_2O_2 [46]. In the aging mice of this study, the RBC and hepatic TBARS and H_2O_2 levels increased compared to YC, and the RBC GSH, hepatic CAT, and GSH-Px activities decreased, which is consistent with reported oxidative stress markers in hepatic steatosis. In all APH supplementation groups, RBC TBARS and hepatic H_2O_2 levels decreased. In contrast, hepatic CAT and GSH-Px activities increased in the LP group, and RBC GSH activity increased in the HP group.

Overall, APH supplementation reduced the visceral fat, a prominent feature of aging, which was positively correlated with decreased insulin resistance and increased glucose utilization. Such efficacy was followed by the inhibition of hepatic steatosis and oxidative stress. Furthermore, high-dose protein supplementation may not be necessary because there was little difference in the effect depending on the APH dose.

In conclusion, APH supplementation reduced visceral fat accumulation and suppressed obesity-related metabolic diseases, including insulin resistance and hepatic steatosis in aged mice. Therefore, the high-quality animal protein APH, which reduces the molecular weight and enhances PDCAAS, highlights its potential as a dietary supplement for healthy aging.

SUPPLEMENTARY MATERIAL

Supplementary Fig. 1
Effect of APH on gastrocnemius muscle glycogen (A), mRNA expression of PRKAA2 on the gastrocnemius muscle (B), mRNA expression related to glucose metabolism on gastrocnemius muscle (C) in aged mice. The data are expressed as the mean ± SEM; Student's *t*-test (n = 4–8).

REFERENCES

1. Guo J, Huang X, Dou L, Yan M, Shen T, Tang W, Li J. Aging and aging-related diseases: from molecular mechanisms to interventions and treatments. Signal Transduct Target Ther 2022;7:391.   **PUBMED | CROSSREF**

2. Kuk JL, Saunders TJ, Davidson LE, Ross R. Age-related changes in total and regional fat distribution. Ageing Res Rev 2009;8:339-48.   **PUBMED | CROSSREF**

3. Jura M, Kozak LP. Obesity and related consequences to ageing. Age (Dordr) 2016;38:23.   **PUBMED | CROSSREF**

4. Folsom AR, Kaye SA, Sellers TA, Hong CP, Cerhan JR, Potter JD, Prineas RJ. Body fat distribution and 5-year risk of death in older women. JAMA 1993;269:483-7.   **PUBMED | CROSSREF**

5. Brochu M, Tchernof A, Dionne IJ, Sites CK, Eltabbakh GH, Sims EA, Poehlman ET. What are the physical characteristics associated with a normal metabolic profile despite a high level of obesity in postmenopausal women? J Clin Endocrinol Metab 2001;86:1020-5.   **PUBMED | CROSSREF**

6. Gan L, Chitturi S, Farrell GC. Mechanisms and implications of age-related changes in the liver: nonalcoholic Fatty liver disease in the elderly. Curr Gerontol Geriatr Res 2011;2011:831536.   **PUBMED | CROSSREF**

7. McGarry JD. What if Minkowski had been ageusic? An alternative angle on diabetes. Science 1992;258:766-70.   **PUBMED | CROSSREF**

8. Lytrivi M, Castell AL, Poitout V, Cnop M. Recent insights into mechanisms of β-cell lipo- and glucolipotoxicity in type 2 diabetes. J Mol Biol 2020;432:1514-34.   **PUBMED | CROSSREF**

9. Fonseca SG, Gromada J, Urano F. Endoplasmic reticulum stress and pancreatic β-cell death. Trends Endocrinol Metab 2011;22:266-74. **PUBMED** | **CROSSREF**

10. Paddon-Jones D, Rasmussen BB. Dietary protein recommendations and the prevention of sarcopenia. Curr Opin Clin Nutr Metab Care 2009;12:86-90. **PUBMED** | **CROSSREF**

11. Bartali B, Frongillo EA, Stipanuk MH, Bandinelli S, Salvini S, Palli D, Morais JA, Volpato S, Guralnik JM, Ferrucci L. Protein intake and muscle strength in older persons: does inflammation matter? J Am Geriatr Soc 2012;60:480-4. **PUBMED** | **CROSSREF**

12. Hackney KJ, Trautman K, Johnson N, Mcgrath R, Stastny S. Protein and muscle health during aging: benefits and concerns related to animal-based protein. Anim Front 2019;9:12-7. **PUBMED** | **CROSSREF**

13. Lim MT, Pan BJ, Toh DW, Sutanto CN, Kim JE. Animal protein versus plant protein in supporting lean mass and muscle strength: a systematic review and meta-analysis of randomized controlled trials. Nutrients 2021;13:661. **PUBMED** | **CROSSREF**

14. Schaafsma G. Advantages and limitations of the protein digestibility-corrected amino acid score (PDCAAS) as a method for evaluating protein quality in human diets. Br J Nutr 2012;108 Suppl 2:S333-6. **PUBMED** | **CROSSREF**

15. Carroll NV, Longley RW, Roe JH. The determination of glycogen in liver and muscle by use of anthrone reagent. J Biol Chem 1956;220:583-93. **PUBMED** | **CROSSREF**

16. Bentle LA, Lardy HA. Interaction of anions and divalent metal ions with phosphoenolpyruvate carboxykinase. J Biol Chem 1976;251:2916-21. **PUBMED** | **CROSSREF**

17. Alegre M, Ciudad CJ, Fillat C, Guinovart JJ. Determination of glucose-6-phosphatase activity using the glucose dehydrogenase-coupled reaction. Anal Biochem 1988;173:185-9. **PUBMED** | **CROSSREF**

18. Davidson AL, Arion WJ. Factors underlying significant underestimations of glucokinase activity in crude liver extracts: physiological implications of higher cellular activity. Arch Biochem Biophys 1987;253:156-67. **PUBMED** | **CROSSREF**

19. Nepokroeff CM, Lakshmanan MR, Porter JW. Fatty-acid synthase from rat liver. Methods Enzymol 1975;35:37-44. **PUBMED** | **CROSSREF**

20. Markwell MA, McGroarty EJ, Bieber LL, Tolbert NE. The subcellular distribution of carnitine acyltransferases in mammalian liver and kidney. A new peroxisomal enzyme. J Biol Chem 1973;248:3426-32. **PUBMED** | **CROSSREF**

21. Lazarow PB. Assay of peroxisomal beta-oxidation of fatty acids. Methods Enzymol 1981;72:315-9. **PUBMED** | **CROSSREF**

22. Ohkawa H, Ohishi N, Yagi K. Assay for lipid peroxides in animal tissues by thiobarbituric acid reaction. Anal Biochem 1979;95:351-8. **PUBMED** | **CROSSREF**

23. Marklund S, Marklund G. Involvement of the superoxide anion radical in the autoxidation of pyrogallol and a convenient assay for superoxide dismutase. Eur J Biochem 1974;47:469-74. **PUBMED** | **CROSSREF**

24. Aebi H. Catalase *in vitro*. Methods Enzymol 1984;105:121-6. **PUBMED** | **CROSSREF**

25. Paglia DE, Valentine WN. Studies on the quantitative and qualitative characterization of erythrocyte glutathione peroxidase. J Lab Clin Med 1967;70:158-69. **PUBMED**

26. Pinto RE, Bartley W. The effect of age and sex on glutathione reductase and glutathione peroxidase activities and on aerobic glutathione oxidation in rat liver homogenates. Biochem J 1969;112:109-15. **PUBMED** | **CROSSREF**

27. Graham A, Hassall DG, Rafique S, Owen JS. Evidence for a paraoxonase-independent inhibition of low-density lipoprotein oxidation by high-density lipoprotein. Atherosclerosis 1997;135:193-204. **PUBMED** | **CROSSREF**

28. Gabriely I, Ma XH, Yang XM, Atzmon G, Rajala MW, Berg AH, Scherer P, Rossetti L, Barzilai N. Removal of visceral fat prevents insulin resistance and glucose intolerance of aging: an adipokine-mediated process? Diabetes 2002;51:2951-8. **PUBMED** | **CROSSREF**

29. Kim YW, Kim JY, Lee SK. Surgical removal of visceral fat decreases plasma free fatty acid and increases insulin sensitivity on liver and peripheral tissue in monosodium glutamate (MSG)-obese rats. J Korean Med Sci 1999;14:539-45. **PUBMED** | **CROSSREF**

30. Jiang Y, Zhang Y, Jin M, Gu Z, Pei Y, Meng P. Aged-related changes in body composition and association between body composition with bone mass density by body mass index in chinese han men over 50-year-old. PLoS One 2015;10:e0130400. **PUBMED** | **CROSSREF**

31. Short KR, Vittone JL, Bigelow ML, Proctor DN, Nair KS. Age and aerobic exercise training effects on whole body and muscle protein metabolism. Am J Physiol Endocrinol Metab 2004;286:E92-101. **PUBMED** | **CROSSREF**

32. Huffman DM, Barzilai N. Role of visceral adipose tissue in aging. Biochim Biophys Acta 2009;1790:1117-23. **PUBMED** | **CROSSREF**

33. Tan CY, Vidal-Puig A. Adipose tissue expandability: the metabolic problems of obesity may arise from the inability to become more obese. Biochem Soc Trans 2008;36:935-40.   **PUBMED** | **CROSSREF**

34. Slawik M, Vidal-Puig AJ. Lipotoxicity, overnutrition and energy metabolism in aging. Ageing Res Rev 2006;5:144-64.   **PUBMED** | **CROSSREF**

35. Rudman D, Feller AG, Cohn L, Shetty KR, Rudman IW, Draper MW. Effects of human growth hormone on body composition in elderly men. Horm Res 1991;36 Suppl 1:73-81.   **PUBMED** | **CROSSREF**

36. Navale AM, Paranjape AN. Glucose transporters: physiological and pathological roles. Biophys Rev 2016;8:5-9.   **PUBMED** | **CROSSREF**

37. Han HS, Kang G, Kim JS, Choi BH, Koo SH. Regulation of glucose metabolism from a liver-centric perspective. Exp Mol Med 2016;48:e218.   **PUBMED** | **CROSSREF**

38. Li X, Sui Y, Wu Q, Xie B, Sun Z. Attenuated mTOR signaling and enhanced glucose homeostasis by dietary supplementation with lotus seedpod oligomeric procyanidins in streptozotocin (STZ)-induced diabetic mice. J Agric Food Chem 2017;65:3801-10.   **PUBMED** | **CROSSREF**

39. Cornu M, Albert V, Hall MN. mTOR in aging, metabolism, and cancer. Curr Opin Genet Dev 2013;23:53-62.   **PUBMED** | **CROSSREF**

40. Chen Z, Yu Y, Cai J, Li H. Emerging molecular targets for treatment of nonalcoholic fatty liver disease. Trends Endocrinol Metab 2019;30:903-14.   **PUBMED** | **CROSSREF**

41. Chen Z, Tian R, She Z, Cai J, Li H. Role of oxidative stress in the pathogenesis of nonalcoholic fatty liver disease. Free Radic Biol Med 2020;152:116-41.   **PUBMED** | **CROSSREF**

42. Friedman SL, Neuschwander-Tetri BA, Rinella M, Sanyal AJ. Mechanisms of NAFLD development and therapeutic strategies. Nat Med 2018;24:908-22.   **PUBMED** | **CROSSREF**

43. Koliaki C, Szendroedi J, Kaul K, Jelenik T, Nowotny P, Jankowiak F, Herder C, Carstensen M, Krausch M, Knoefel WT, et al. Adaptation of hepatic mitochondrial function in humans with non-alcoholic fatty liver is lost in steatohepatitis. Cell Metab 2015;21:739-46.   **PUBMED** | **CROSSREF**

44. Videla LA, Rodrigo R, Orellana M, Fernandez V, Tapia G, Quiñones L, Varela N, Contreras J, Lazarte R, Csendes A, et al. Oxidative stress-related parameters in the liver of non-alcoholic fatty liver disease patients. Clin Sci (Lond) 2004;106:261-8.   **PUBMED** | **CROSSREF**

45. Köroğlu E, Canbakan B, Atay K, Hatemi İ, Tuncer M, Dobrucalı A, Sonsuz A, Gültepe I, Şentürk H. Role of oxidative stress and insulin resistance in disease severity of non-alcoholic fatty liver disease. Turk J Gastroenterol 2016;27:361-6.   **PUBMED** | **CROSSREF**

46. Masarone M, Rosato V, Dallio M, Gravina AG, Aglitti A, Loguercio C, Federico A, Persico M. Role of oxidative stress in pathophysiology of nonalcoholic fatty liver disease. Oxid Med Cell Longev 2018;2018:9547613.   **PUBMED** | **CROSSREF**